A Computational Study on the Mechanism and Kinetics of the Pyrolysis of 2-Nitrophenyl Azide

Guntram Rauhut* and Frank Eckert

Universität Stuttgart, Institut für Theoretische Chemie, Pfaffenwaldring 55, 70569 Stuttgart, Germany

Received: April 8, 1999; In Final Form: August 9, 1999

The thermolysis of *ortho*-nitrophenyl azide, yielding benzofuroxan and nitrogen, has been investigated using quantum chemical methods up to the CCSD(T)/6-311G(2d,p) level. The calculated activation barriers are in excellent agreement with experimental data. A comparison of the rate constants computed from various implementations of variational transition state theory with experimental data clearly identifies the computed reaction mechanism as the experimentally observed one. Neighboring-group assistance within the pyrolysis leads to a one-step mechanism, thus turning down intermediates as discussed in the literature.

Introduction

The pyrolysis of *ortho*-substituted aryl azides is a standard route for synthesizing 1,2,5-oxadiazoles fused to aromatic or heterocyclic rings. The products of these reactions are an important class of heterocyclic compounds with highly interesting biochemical and pharmacological properties (for an overview, see refs 1−5). Many phenyl azides with unsaturated *ortho*-substituents can be pyrolyzed in order to yield cyclic products following the general scheme depicted in Figure 1. Experimental studies on the reaction rates of the pyrolysis of a large number of substituted phenyl azides show that the formation of a delocalized heterocyclic ring system can be regarded as the driving force for this reaction.[6−10] For the compounds under consideration, a clean first-order kinetic behavior has been reported.[6−9,11−13] The reaction rates of pure liquid azides differ only slightly from the rates in solution. The latter are invariant with respect to the nature of the solvent used in the experimental measurements, suggesting little or no specific solvation effects between the solvent and the phenyl azides.[11] In addition, the experimental results indicate that the reaction proceeds without any side reactions: the sum of the concentrations of the reactant and the products is reported to remain constant throughout the kinetic measurements.[7,9,11] The absence of side reactions as well as the fact that a negative value for the entropy of activation is found for almost all compounds measured experimentally[9,10] both indicate the presence of a cyclic transition state. Thus, a concerted one-step mechanism is proposed by a number of groups.[6,7,9,11,14] However, different reaction mechanisms via stable cyclic intermediates have also been discussed.[2,8,12]

The pyrolysis of 2-nitrophenyl azide **1**, yielding benzofuroxan **2** and nitrogen can be considered a prototype for this class of reactions. Figure 2 shows the one-step mechanism proposed for this reaction, proceeding via a planar transition state **TS1**. Figure 3 shows the stable intermediate structures that were also discussed for the reaction of **1**, namely, a nitrenic structure **I1**,[2,8] a bridged intermediate **I2**,[2,8,9] a cyclic structure **I3**,[8] and an intermediate **I4**[2] which is structurally similar to transition state **TS1**. It has been pointed out, however, that the existence of intermediates **I2** and **I3** will only be likely in special cases, such as the pyrolysis of 2-azido-benzophenones (see Figure 1, *X*═*Y*: benzoyl).[8,9]

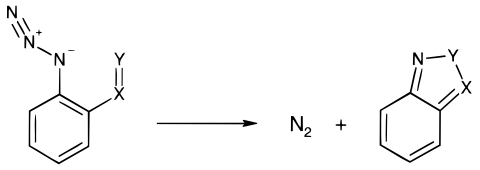

Figure 1. Pyrolysis of *ortho*-substituted phenyl azides. *X*═*Y*: nitro, phenylazo, acetyl, or benzoyl.

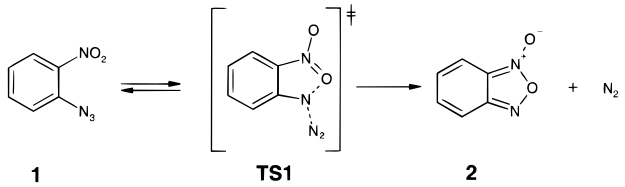

Figure 2. Concerted mechanism of the pyrolysis of 2-nitrophenyl azide.

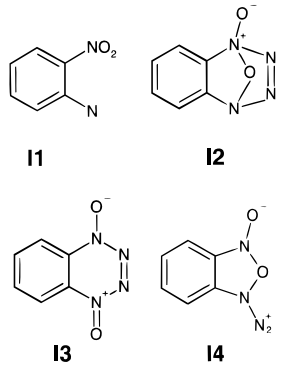

Figure 3. Possible intermediates involved in the pyrolysis of 2-nitrophenyl azide.

This paper attempts to clarify the mechanism of the *ortho*-assisted pyrolysis of phenyl azides from a computational point of view. No quantum chemical calculations have yet been reported on this reaction.

Computational Details

Previous studies on the Boulton−Katritzky rearrangement of substituted benzofuroxans[15,16] showed that very high levels of

* To whom correspondence should be addressed. E-mail: rauhut@theochem.uni-stuttgart.de.

10.1021/jp991181y CCC: $18.00
Published on Web 10/26/1999

TABLE 1: Geometric Parameters of 2-Nitrophenyl Azide 1 (C_1)

r^a	MP2	B3-LYP	∠	MP2	B3-LYP
C_1-C_2	1.403	1.410	$C_1-C_2-C_3$	121.8	121.1
C_2-C_3	1.392	1.395	$C_2-C_3-C_4$	119.4	120.4
C_3-C_4	1.393	1.389	$C_3-C_4-C_5$	119.7	119.3
C_4-C_5	1.397	1.398	$C_4-C_5-C_6$	120.5	120.5
C_5-C_6	1.394	1.390	$C_5-C_6-C_1$	120.6	121.1
C_6-C_1	1.403	1.406	$C_6-C_1-C_2$	118.0	117.7
C_1-N_1	1.412	1.406	$N_1-C_1-C_2$	118.4	119.6
N_1-N_2	1.245	1.239	$N_2-N_1-C_1$	117.0	118.1
N_2-N_3	1.164	1.140	$N_3-N_2-N_1$	171.9	171.3
C_2-N_4	1.461	1.471	$C_1-C_2-N_4$	120.7	122.3
N_4-O_1	1.243	1.223	$C_2-N_4-O_1$	117.6	118.4
N_4-O_2	1.244	1.233	$C_2-N_4-O_2$	116.8	116.8
C_3-H_2	1.085	1.083	$C_4-C_3-H_2$	121.8	121.6
C_4-H_3	1.086	1.085	$C_3-C_4-H_3$	119.9	120.0
C_5-H_4	1.087	1.086	$C_4-C_5-H_4$	120.2	120.3
C_6-H_5	1.088	1.086	$C_1-C_6-H_5$	119.5	119.1
			$C_1-C_2-N_4-O_1$	40.7	25.9

[a] Bond lengths are in ångstrøms and angles in degrees.

ab initio theory need to be applied for a reliable description of these compounds. While geometries are properly reproduced at the B3-LYP level, energies may not be. For this reason, on top of all B3-LYP optimized geometries, CCSD and CCSD(T) single-point calculations in combination with a 6-311G(2d,p) basis were performed, which can be considered to be sufficiently accurate as discussed recently.[15] This working scheme results in approximately 3×10^7 configuration state functions at the CCSD level. For geometry optimizations, a comparably small 6-31G* basis was used, but again, previous studies showed that changes in geometries due to basis set effects are much smaller than those due to an improper treatment of electron correlation. For comparison purposes, geometries were also optimized at the MP2 level.

The potential energy surface (PES) of the system was scanned systematically for all intermediate and transition structures mentioned above. Stationary points found on the PES were optimized tightly, allowing a maximum of 1×10^{-5} au for each gradient component. Force constants were calculated at the optimized geometries, allowing the assignment of stationary points as minima or transition states and the determination of the zero-point vibrational energies (ZPEs) at these geometries. Transition states were verified by following the minimum energy path (MEP) towards the reactant and product minima.

All MP2 and CCSD(T) calculations were carried out with the Molpro quantum chemistry package,[17] using the default optimization[18] and MEP following algorithms.[19] The B3-LYP[20] density functional theory calculations were carried out with the G94 program[21] using the default optimizer and MEP following algorithms.[22] Consequently, the B3-LYP hybrid functional used incorporates the VWN functional III of Vosko, Wilk, and Nusair[23] and not their recommended functional V, which is the usual choice.

Reaction Mechanisms

Geometries. Table 1 shows the geometries of 2-nitrophenyl azide **1** optimized at the B3-LYP/6-31G* and MP2/6-31G* levels, respectively. The labeling of the atoms is given in Figure 4. Differences between the predicted geometries of the two methods are small, the largest difference of 0.024 au being in the N_2-N_3 bond of the azido group. Note that both methods predict the nitro group being twisted out of the ring plane, indicating sterical hindrance between the nitro and the azido group. A planar conformer, being only less than 0.2 kcal/mol (B3-LYP) higher in energy, was identified as a saddle point of the rotation of the nitro group. This indicates a very shallow potential and readily explains the rather large differences of the corresponding torsional angles (cf. Table 1) between the MP2 and B3-LYP geometries.

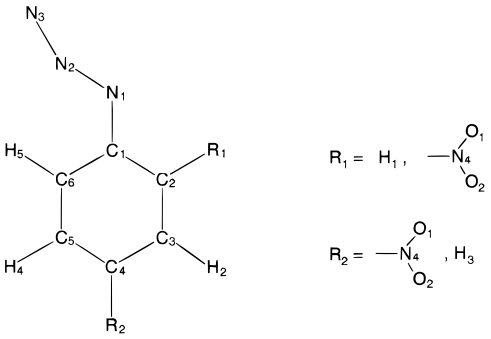

Figure 4. Atom labeling of 2- and 4-nitrophenyl azide.

Since experimental X-ray data are not available for **1** but are available for the corresponding para isomer,[24] additional calculations were carried out for this molecule. Table 2 shows a comparison between the experimental data and the geometries optimized at the B3-LYP/6-31G* and MP2/6-31G* levels. Again, B3-LYP and MP2 geometries closely resemble each other. The largest deviations relative to the experimental values are in the C−C distances of the aromatic ring. However, the standard deviations of the experimental measurements are also quite large for these bonds. For this compound, which of course does not show steric interactions between the azido and the nitro group, theory as well as experiment predict a planar structure (C_s symmetry). The azido group is predicted to be slightly bent, with 172 degrees in very good agreement with experiment. The same is found for the ortho isomer. Since the structure of *para*-nitrophenyl azide is reliably reproduced by both methods, the same can be expected for the corresponding structure of the ortho isomer.

As reported previously,[25] the structure of benzofuroxan is nicely reproduced at the B3-LYP level, while MP2 fails in the description of the endocyclic $N^+ -O$ bond. This bond, which is known to be particularly sensitive to dynamical electron correlation, is reliably reproduced either at the B3-LYP or the MP4(SDQ) level only. This study solely relies on the less demanding B3-LYP results. The resulting van der Waals (vdW) complex of benzofuroxan and nitrogen in the exit channel of the reaction is discussed in detail below.

The Concerted Reaction Mechanism. The concerted mechanism shown in Figure 2 affects the π-bonds throughout the molecule. Note that benzofuroxan must be considered an *ortho*-quinoide system with a pronounced bond alternation, and thus the π-system of the benzene ring rearranges as well. The shifting of the π-bonds requires that the azido and the neighboring nitro group are in the plane of the aromatic ring. This is reproduced by the theoretical calculations, which predicted a planar transition state **TS1**. Figure 5 shows the geometry of transition state **TS1**, optimized at the B3-LYP/6-31G* level. The optimized MP2/6-31G* values are given in parentheses. The relatively short N_1-O_1 distance (2.071 Å) indicates a non-negligible interaction between N_1 and the nitro group (i.e., the furoxan ring is already preformed). This is further supported by a significantly shorter C_2-N_4 distance (i.e., the bond between the nitro group and the benzene ring, $\Delta r = 0.058$) in the transition state than in the educt. The bond alternation of the six-membered ring in **TS1** is already as strong as in the product (B3-LYP: 1.379 Å vs 1.425 Å). B3-LYP and MP2 predict a substantially different

TABLE 2: Geometric Parameters of 4-Nitrophenyl Azide 3 (C_s)

r^a	MP2	B3-LYP	exp[b]	∠	MP2	B3-LYP	exp.[b]
C_1-C_2	1.401	1.404	1.374(18)	$C_1-C_2-C_3$	119.9	120.1	120.5(1.2)
C_2-C_3	1.385	1.387	1.390(20)	$C_2-C_3-C_4$	118.9	119.1	117.2(1.3)
C_3-C_4	1.394	1.395	1.391(19)	$C_3-C_4-C_5$	122.1	121.7	123.0(1.3)
C_4-C_5	1.393	1.395	1.370(20)	$C_4-C_5-C_6$	118.8	119.2	118.5(1.2)
C_5-C_6	1.392	1.389	1.378(19)	$C_5-C_6-C_1$	119.8	119.8	120.0(1.2)
C_6-C_1	1.402	1.405	1.386(18)	$C_6-C_1-C_2$	120.5	120.2	120.7(1.2)
C_1-N_1	1.417	1.412	1.417(17)	$N_1-C_1-C_2$	115.7	115.7	115.0(1.1)
N_1-N_2	1.247	1.241	1.270(16)	$N_2-N_1-C_1$	117.4	118.4	115.0(1.0)
N_2-N_3	1.164	1.139	1.127(17)	$N_3-N_2-N_1$	172.4	172.2	173.4(1.3)
C_4-N_4	1.467	1.466	1.447(19)	$C_3-C_4-N_4$	119.1	119.2	117.7(1.3)
N_4-O_1	1.242	1.231	1.229(16)	$C_4-N_4-O_1$	117.6	117.7	119.7(1.1)
N_4-O_1	1.243	1.232	1.251(15)	$C_4-N_4-O_2$	117.6	117.7	119.0(1.1)
C_2-H_1	1.086	1.086	(0.98)	$C_1-C_2-H_1$	119.0	119.0	(121)
C_3-H_2	1.089	1.083	(0.98)	$C_4-C_3-H_2$	119.6	119.5	(118)
C_5-H_4	1.085	1.083	(1.09)	$C_4-C_5-H_4$	119.9	119.5	(124)
C_6-H_5	1.088	1.086	(1.09)	$C_1-C_6-H_5$	120.6	120.4	(117)

[a] Bond lengths are in ångstrøms and angles in degrees. [b] Mugnoli et al. ref 24. Estimated standard deviations for experimental values are given in parentheses.

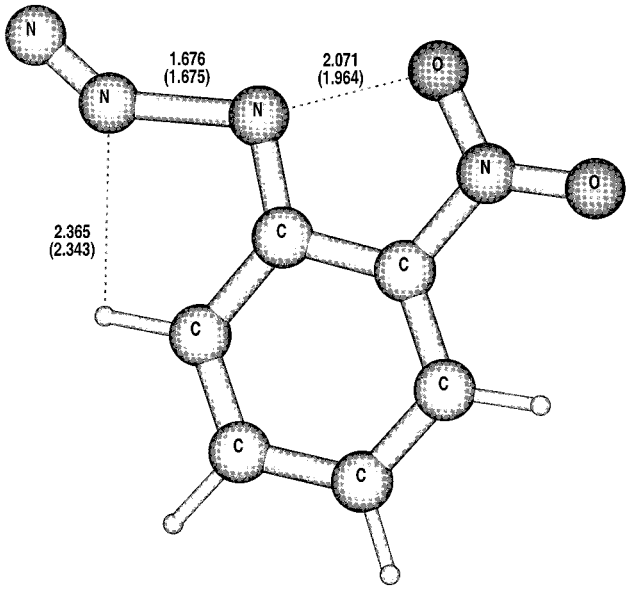

Figure 5. Transition-state geometry of the pyrolysis of 2-nitrophenyl azide optimized at the B3-LYP/6-31G* level. Distances are in [Å], and MP2/6-31G* values are given in parentheses.

N_1-O_1 distance in **TS1**. The difference of $\Delta r > 0.1$ Å is much larger than for any of the bonds in **1**. A similar tendency was reported previously for the transition state of the Boulton−Katritzky rearrangement of 4-nitrobenzofuroxan.[15] In this reaction, MP2 predicts an N−O bond length in the transition state also being about 0.1 Å shorter than the corresponding B3-LYP value, the latter being essentially identical with an MP4(SDQ) bond length. Moreover, compared to experimental values, MP2 underestimates the N_1-O_1 in benzofuroxans by about 0.06 Å, while B3-LYP is in good agreement.[25] From these results, one must conclude that the MP2 method does not cover a sufficient amount of electron correlation for a proper description of these structures. Consequently, the B3-LYP geometry of the transition state must be considered to be of higher quality.

Relative energies for all species involved in the concerted reaction path are given in Table 3. The CCSD(T) values which must be considered most reliable are nicely reproduced by the B3-LYP energies. However, this favorable result must be considered accidental, since it has been shown by several groups that the B3-LYP functional systematically underestimates reaction barriers.[26,27] As will be discussed in detail below, the agreement of both methods with experimental data is excellent. As has been stated above, the MP2 energies for **TS1** and **2** must be considered erroneous. Deviations of relative energies with respect to the applied methods are much larger for the resulting vdW complex than for the transition state. This must be addressed to the unusual electronic structure of benzofuroxan.

The Benzofuroxan−Nitrogen Complex. The pyrolysis of 2-nitrophenyl azide formally leads to a vdW complex of benzofuroxan and nitrogen. The structure of this complex is shown in Figure 6. The overestimation of the endocyclic N^+-O bond in benzofuroxan by MP2 is well-known and is discussed in detail in ref 25. Geometric differences between B3-LYP and MP2 for the intermolecular distances are quite significant, but this had to be expected. First of all, the potential energy surface is extremely shallow for these coordinates, and consequently, small energetic differences lead to strong geometric changes. Second, modern density functionals are well-known for their failure in describing dispersion interactions.[28] Thus, the structure of the complex optimized at the B3-LYP level is driven mainly by basis set superposition errors (BSSE) rather than actual physical forces. Since MP2 seizes a certain amount of the dispersion energy, the intermolecular distances shown in Figure 6 are shorter than for B3-LYP, yet BSSE must be expected to have a strong impact on these parameters. To yield more accurate structures, one would need to perform geometry optimizations using local correlation methods in combination with a basis set augmented by diffuse functions.[29] These methods, by nature, eliminate most of the BSSE.[30] However, the strong π-delocalization in benzofuroxans causes convergence problems in the localization procedure, which means that these methods are of limited use for this particular class of molecules. We considered geometry effects on the vdW complexation energy to be very small and therefore did not try to yield most accurate intermolecular distances. Moreover, this study focuses mainly on the reaction mechanism of this reaction and its kinetics, for which the observed vdW complex is of minor importance. Nevertheless, the complexation energy calculated for this cluster is listed in Table 4. BSSE effects are of the same magnitude as the dispersive interactions. The stabilization of the complex must be expected to be in the range of −0.9 kcal/mol. In comparison to the reaction energy as provided in Table 3 the complexation energy is 1 order of magnitude smaller. Consequently, this complex, in practice, will never be observed, since translational excess energy will immediately drive the products apart. As discussed by Truhlar,[31] vdW complexes in the exit channel of a reaction with a

TABLE 3: Calculated Relative Energies[a] of Structures Involved in the Pyrolysis of 2-Nitrophenyl Azide 1

energy		geometry		TS1		2	
method	basis	method	basis	E_{rel}	E_{rel}^{scal}	E_{rel}	E_{rel}^{scal}
B3-LYP	6-31G*	B3-LYP	6-31G*	27.82	25.65	−23.19	−25.22
MP2	6-31G*	MP2	6-31G*	40.34	38.17	−28.51	−31.24
MP2	6-311G(2d,p)	B3-LYP	6-31G*	38.98	36.81	−26.94	−28.97
CCSD	6-311G(2d,p)	B3-LYP	6-31G*	27.23	25.06	−32.16	−34.19
CCSD(T)	6-311G(2d,p)	B3-LYP	6-31G*	26.76	24.59	−31.34	−33.37

[a] Energies [in kcal/mol] are relative to 2-nitrophenyl azide **1**. E_{rel}: Relative energy without correction by ZPEs. E_{rel}^{scal}: Relative energy corrected by scaled ZPEs. B3-LYP, MP2/6-311G(2d,p), CCSD, and CCSD(T) relative energies are corrected by B3-LYP/6-31G*-ZPEs, scaled by a factor of 0.963. MP2/6-31G* relative energies are corrected by MP2/6-31G*-ZPEs, scaled by a factor of 0.943.

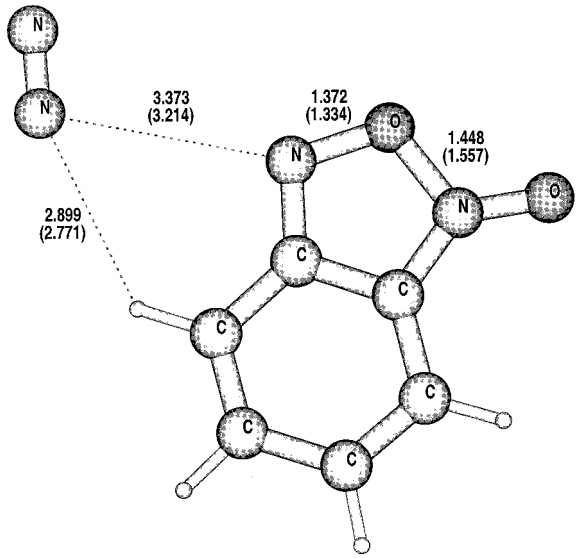

Figure 6. Geometry of the complex of benzofuroxan and nitrogen, optimized at the B3-LYP/6-31G* level. Distances are in [Å], and MP2/6-31G* values are given in parentheses.

TABLE 4: Interaction Energies[a] Between N_2 and Benzofuroxan in the VdW Complex

energy		geometry		interaction	
method	basis	method	basis	ΔE	ΔE^{b}_{CPC}
B3-LYP	6-31G*	B3-LYP	6-31G*	−0.81	−0.14
MP2	6-31G*	MP2	6-31G*	−1.94	−0.91
MP2	6-311G(2d,p)	B3-LYP	6-31G*	−1.85	−1.12
CCSD	6-311G(2d,p)	B3-LYP	6-31G*	−1.42	−0.72
CCSD(T)	6-311G(2d,p)	B3-LYP	6-31G*	−1.60	−0.85

[a] Energies in kcal/mol. [b] Counterpoise corrected interaction energy.

pronounced reaction barrier essentially have no impact on the kinetic data obtained from variational transition state theory (see below). The reaction energy, that is the energy of the complex relative to **1**, varies between −25.2 and −34.2 kcal/mol. This broad scattering is typical for benzofuroxans when described by low-level correlation methods such as MP2. Furthermore, B3-LYP is well-known not only for its proper description of the molecular structure of benzofuroxans but also for its problems in reproducing relative energies of this molecular class.[15,25] For this particular reason, the coupled-cluster results, especially the CCSD(T) energy, must be considered to be the only reliable data.

Alternative Reaction Mechanisms. The intermediate structures of the pyrolysis of **1** as proposed in the literature[2,8,9] (see Figure 3) were optimized at the B3-LYP/6-31G* level. However, in most cases the optimizations did not lead to the desired structures. Either no stable structure at all or only transition states of higher order were found. Systematic scans of the PES of this reaction showed that no stationary point corresponding to structure **I1** exists for the theoretical methods taken into account here. Consequently, all geometry optimizations starting from (singlet) nitrene-like structures rapidly converged toward the structure of **2**. Moreover, no intermediate of the form **I2** could be found from geometry optimizations and PES scans. Instead, a van der Waals complex of nitrogen with *amphi*-1,2-dinitrosobenzene (the nitrogen lying above the ring plane at a distance of 2.4 Å) was optimized. Although the energy of this structure was only 6.5 kcal/mol higher than that of the reactant, it cannot be considered as taking part in the pyrolysis. Note that *amphi*-1,2-dinitrosobenzene is an intermediate of the ring-chain tautomerism in benzofuroxans,[25] a reaction that can be observed as a follow-up reaction of the pyrolysis. The same holds true for the intermediate structure **I3**. Systematic scans of the PES did not indicate the existence of a stationary point on the PES that could be assigned to structure **I3**. Similar to the **I2** case, all optimizations lead to van der Waals complexes of *anti*-1,2-dinitrosobenzene with nitrogen. The only intermediate that was actually found is of the form **I4**, which is structurally related to transition state **TS1**. However, it is energetically much higher (>80 kcal/mol including ZPE corrections).

The main difference between **TS1** and **I4** is the linear structure of the azido group in **I4**, whereas the azido group in **TS1** is bent by ∼30° (see Figure 5). Due to its extremely high relative energy, **I4** cannot be considered a relevant intermediate for the reaction under consideration. Furthermore, it is unlikely that the large energy difference between **I4** and the structures involved in the concerted reaction path will diminish at higher-level ab initio calculations. It must be concluded that the concerted reaction mechanism via **TS1** is the only reasonable pathway for the pyrolysis of **1**. Thus, the following discussions will focus solely on the properties of the structures involved in the concerted reaction path (Figure 2).

TABLE 5: Energies and Entropies of Activation for the Pyrolysis of 2-Nitrophenyl Azide 1[a]

method	E_{act}	ΔS_{act}
B3-LYP	25.7	−2.0
MP2	38.2	−1.4
CCSD(T)	24.6	
experiment[b]	25.5 ± 0.6	−6.9 ± 1.8
experiment[c]	26.2 ± 0.3	−4.9 ± 0.8
experiment[d]	25.7	−5.9
experiment[e]	26.6 ± 0.2	−2.2 ± 0.4

[a] Energies in kcal/mol, entropies in cal/mol K. For theoretical values cf. Table 3. [b] Dyall.[9] [c] Dyall et al.[7] [d] Birkhimer et al.[12] No standard deviations are given. [e] Fagley et al. 11.

Activation Energies and Entropies. Table 5 compares the calculated activation energies and entropies with the experimental values generated from various kinetic measurements. Surprisingly, the calculated B3-LYP barrier was closer to the experimental activation energies than the CCSD(T) value.

However, a systematic comparison of relative reaction energies at the CCSD(T) and B3-LYP levels for a large number of chemical reactions shows that the average deviation of B3-LYP relative energies from experimental values is about twice as large as for CCSD(T).[32] Thus, the favorable B3-LYP results obtained here must be considered as chance. As mentioned above, the B3-LYP method usually underestimates reaction barriers.[26,27] The experimental values of the activation entropy vary substantially between the different measurements (cf. Table 5), making a comparison to the theoretical results quite difficult. Nevertheless, the computed results must be considered as being at the lower limit. As has been pointed out by Dyall,[9] due to the large standard entropy of nitrogen, large fluctuations in ΔS_{act} reflect fairly small variations in the position of the transition state on the reaction coordinate. The main contributions to ΔS_{act} arise from the vibrational parts of the entropy.

As discussed above and shown in Figure 5, deviations in geometric parameters of **TS1** between the methods used are non-negligible and may account for the difficulties associated with the determination of the activation entropy. Thus, the errors of the calculated entropies of activation are mainly due to the harmonic approximation of the calculated force constants and possibly also due to the flaws of the quantum chemical methods or deficiencies of the basis sets used. Unfortunately, the calculation of the activation entropy (involving the optimization of the geometries of the educt and the transition state plus the calculation of force constants at both points) was computationally not feasible at the CCSD(T) level. However, the B3-LYP method is known to reproduce harmonic force constants and ZPEs quite well[33−38] and thus must be considered the most reliable source of activation entropies available here.

Reaction Rates

Reaction rates were calculated using the canonical variant of variational transition state theory (VTST).[39] Quantum effects (tunneling) were included a posteriori using the semiclassical small curvature tunneling (SCT) correction.[39] The minimum energy path (MEP) of the reaction considered here, that is the pyrolysis of 2-nitrophenyl azide **1**, was interpolated from the geometries, the energy, the gradient, and Hessian information at all three stationary points plus one additional point on each side of the transition state using interpolated VTST by mapping (IVTST-M).[40] The additional point on the MEP was chosen at a distance of $s = \pm 0.1$ amu$^{1/2}$ a_0 from the saddle point. Moreover, two more points were computed at a distance of $s = \pm 0.3$ amu$^{1/2}$ a_0, but Hessians were not evaluated for these structures. Consequently, this results in an IVTST-M-2/4 procedure with two more gradient points than Hessians, as recommended by Corchado et al.[40] Geometries, energies, gradients, and Hessians at these points were obtained from B3-LYP/6-31G* calculations. Additionally, another IVTST-M calculation was performed that utilized B3-LYP/6-31G* geometries, gradients, and Hessians but used CCSD(T)/6-311G(2d,p) energies. To obtain an estimate of the importance of recrossing effects at the reaction barrier, conventional transition-state theory (TST) was also used to compute rate constants.

For a temperature of 1500 K, the canonical variational transition state is positioned on the MEP at $s = -0.45$ amu$^{1/2}$ a_0 for B3-LYP/IVTST-M and at $s = -0.44$ amu$^{1/2}$ a_0 for CCSD(T)/IVTST-M. At lower temperatures, it is considerably closer to the classical transition state (at 300 K they are positioned at $s = -0.02$ and $s = -0.03$ amu$^{1/2}$ a_0 for B3-LYP/IVTST-M and CCSD(T)/IVTST-M, respectively). These comparably large shifts explain the differences between the measured and computed values of ΔS_{act} (see above). We consider the shifts of the transition states at high temperatures estimates rather than exact values, since the number of Hessians and gradient points (2/4) is very small. Additional points certainly would lead to an improved interpolation, but due to the computational demands of the electronic structure calculations, this was out of range for the reaction under investigation. It is notable here that the CCSD(T) curves of the classical potential energy, V_{MEP}, and the corresponding vibrationally adiabatic ground-state potential energy, V_a^G, do not only differ from the B3-LYP curves with respect to the barrier height, but also in their shape and curvature. Since the nonstationary points along the MEP differ significantly with respect to their relative energy, this must be expected. For instance, the structure at $s = -0.3$ amu$^{1/2}$ a_0 is lower in energy than the corresponding structure on the other side ($s = +0.3$ amu$^{1/2}$ a_0) at the B3-LYP level, while the opposite is true at CCSD(T) level. As shown above, due to the correlation-sensitive wave function of the product (benzofuroxan), the reaction energy is much higher (−33.4 kcal/mol, see Table 3) at the CCSD(T) level than that obtained from the B3-LYP functional (−25.2 kcal/mol) which consequently also affects the nonstationary points along the MEP. This indicates that the dynamics of the reaction might be described differently by the two theoretical methods.

The antisymmetric stretching mode of the azido group is rapidly shifted in the region of the classical transition state ($\Delta\nu > 150$ cm^{-1} in the range from $s = -0.1$ amu$^{1/2}$ a_0 to $s = +0.1$ amu$^{1/2}$ a_0), reflecting the spatial separation of nitrogen once the reaction has passed over the reaction barrier. This again explains the difficulties associated with the correct determination of the activation entropy. The relatively small region where the large change of this mode occurs again stresses the importance of an accurately optimized transition state as obtained from the electronic structure calculation. Deviations in the transition state geometry or in the geometry of the additional MEP points for the IVTST-M calculation can thus impose large errors on the projected normal modes under consideration (cf refs 19−41). In IVTST calculations, frequencies are interpolating by sorting them according to canonical order, which often results in an incorrect correlation of the active modes. Therefore, the assignment of the modes along the MEP has been based on the total energy distribution technique (**M**-matrix).[42,43] From this procedure, other important modes with strong changes along the path were identified. Not unexpectedly, a particularly important one is the symmetric stretching mode of the nitro group at 1402 cm^{-1}. This particular mode must be correlated with the endocyclic NO-stretching observed in the benzofuroxan complex at 487 cm^{-1},[44] indicating a significant redistribution of the vibrational energy. Shifts of about 100 cm^{-1} can be observed for ring deformations and ring torsional modes, confirming the importance of the intramolecular shifting of the π-bonds for the reaction rate, as already pointed out by Dyall and Kemp.[7] Unfortunately, the advantage of the **M**-matrix technique could not be utilized for the evaluation of the effective reduced mass needed for the small-curvature tunneling (SCT) correction. Since this quantity is a function of the normal-mode turning points and their derivatives, the SCT transmission coefficients must be considered with great care.[45]

Table 6 compares the rate constants of the pyrolysis of **1** computed at different levels of transition state theory and ab initio theory with the experimental values of Dyall.[9] The computed rate constants are consistently larger than the experimentally obtained ones. Moreover, CCSD(T) rate constants are larger than B3-LYP values. Since the classical activation barrier

TABLE 6: Rate Constants for the Pyrolysis of 2-Nitrophenyl Azide 1[a]

method	$T = 345.2$ K	$T = 359.4$ K	$T = 370.3$ K
B3-LYP/TST	2.0×10^{-4}	9.0×10^{-4}	2.7×10^{-3}
CCSD(T)/TST	4.7×10^{-4}	2.1×10^{-3}	5.9×10^{-3}
B3-LYP/IVTST-M	1.4×10^{-4}	6.2×10^{-4}	1.8×10^{-3}
CCSD(T)/IVTST-M	2.6×10^{-4}	1.2×10^{-3}	3.4×10^{-3}
B3-LYP/IVTST-M/SCT	7.9×10^{-4}	3.2×10^{-3}	8.6×10^{-3}
CCSD(T)/IVTST-M/SCT	1.4×10^{-3}	5.7×10^{-3}	1.5×10^{-2}
experiment[b]	4.2×10^{-5}	1.9×10^{-4}	5.4×10^{-4}
experiment[c]		2.4×10^{-4}	8.1×10^{-4}
experiment[d]	8.6×10^{-5}	1.5×10^{-4}	3.9×10^{-4}
experiment[e]	4.7×10^{-5}	2.2×10^{-4}	

[a] Rate constants k in 1/s. See text for explanation of abbreviations. [b] Dyall,[9] measured in decalin solution (0.01 M). [c] Dyall et al.,[7] measured in decalin solution (0.2 M) at T=360.2 and 372.6 K. [d] Birkhimer et al.,[12] measured in di-*n*-butyl-phthalate solution (0.1 M) at $T = 349.4$, 354.9, and 364.0 K. [e] Fagley et al.,[11] measured in heptane solution (4.9×10^{-5} M) at $T = 344.9$ K and in di-*n*-butylphthalate solution (0.12 M) at $T = 357.6$ K, respectively.

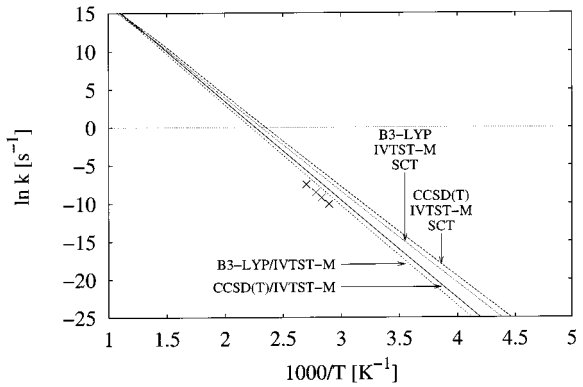

Figure 7. Arrhenius-plot of the rate constants of the pyrolysis of 2-nitrophenyl azide. The (×) symbols denote the experimental values of Dyall.[9]

is lower at the CCSD(T) level (cf. Table 5), this trend had to be expected. In best agreement with Dyall's data are the B3-LYP/IVTST-M values, revealing the excellent agreement of the classical activation barrier between B3-LYP and experimental results. Nevertheless, this must be considered as chance, while the CCSD(T) results are of higher quality. Variational TST leads to a slight correction of the rate constants relative to conventional TST. At the CCSD(T) level, recrossing effects are more strongly pronounced than at the B3-LYP level and lower the rate constants by a factor of almost 1/2. Tunneling effects, represented by the SCT transmission coefficient, lead to a significant overestimation of the computed rate constants. As mentioned above, the problem of correlating the generalized frequencies correctly within the framework of IVTST theory may lead to certain errors in the effective reduced mass. As already pointed out by Truhlar et al.,[31] this may lead to an overestimation of the tunneling correction. Consequently, IVTST rates including SCT corrections are often less reliable than IVTST rates without tunneling corrections (as long as the reaction is not determined by tunneling effects). Since one would not expect significant tunneling contributions for the reaction investigated here, we address the effect observed here mainly to be an artifact of the IVTST methodology rather than being of true physical nature. Therefore, we consider the IVTST-M calculations presented here more accurate than the IVTST-M/SCT values. Figure 7 shows an Arrhenius plot of the rate constants. In addition, the experimental values of Dyall are depicted.

Summary and Conclusions

The reaction mechanism of the pyrolysis of 2-nitrophenyl azide toward benzofuroxan was investigated at the B3-LYP, MP2, and CCSD(T) levels. MP2 fails to describe the reaction reliably. In agreement with experimental data, all methods predict a one-step mechanism via a planar transition state that already shows a partial bond between one oxygen atom of the nitro group and the azido group. In the exit channel of the reaction, a weakly bonded van der Waals complex was found, but due to the strong exothermicity of the reaction, this complex is unlikely to be trapped experimentally. Intermediates as discussed in the literature could not be found or were identified to be irrelevant for the reaction mechanism. The computed CCSD(T) and B3-LYP activation barriers are in excellent agreement with experimental data. Computed rate constants show slightly larger errors than those reported for smaller systems but are still in good agreement with the experimental data obtained by several groups.

Acknowledgment. Computer time on the SGI PowerChallenge of the Institut für Theoretische Chemie (Stuttgart) and on the NEC SX-4 of the HLRS Stuttgart is kindly acknowledged. We thank Prof. D. Truhlar for helpful suggestions and for providing us with a copy of the Polyrate program.

References and Notes

(1) Paton, R. M. 1,2,5-Oxodiazoles. In *Comprehensive Heterocyclic Chemistry II*, Vol. 4; Katritzky, A. R., Ed.; Pergamon Press: New York, 1996.
(2) Friedrichsen, W. Arenofurazan-1-oxide. In *Houben-Weyl, Methoden der Organischen Chemie*, Vol. E8c; Schaumann, E., Ed.; Thieme: Stuttgart, 1994.
(3) Gasco, A.; Boulton, A. J. *Adv. Heterocycl. Chem.* **1981**, *29*, 251.
(4) Ghosh, P. B.; Ternai, B.; Whitehouse, M. W. *Med. Res. Rev.* **1981**, *1*, 159.
(5) Boulton, A. J.; Ghosh, P. B. *Adv. Heterocycl. Chem.* **1969**, *10*, 1.
(6) Patai, S.; Gotshal, Y. *J. Chem. Soc. (B)* **1966**, 489.
(7) Dyall, L. K.; Kemp, J. E. *J. Chem. Soc. (B)* **1968**, 976.
(8) Hall, J. H.; Behr, F. E.; Reed, R. L. *J. Am. Chem. Soc.* **1972**, *94*, 4952.
(9) Dyall, L. K. *Aust. J. Chem.* **1975**, *28*, 2147.
(10) Dyall, L. K. *Aust. J. Chem.* **1977**, *30*, 2669.
(11) Fagley, T. F.; Sutter, J. R.; Oglukian, R. L. *J. Am. Chem. Soc.* **1956**, *78*, 5567.
(12) Birkhimer, E. A.; Norup, B.; Bak, T. A. *Acta Chem. Scand.* **1960**, *14*, 1894.
(13) Andersen, E.; Birkhimer, E. A.; Bak, T. A. *Acta Chem. Scand.* **1960**, *14*, 1899.
(14) Chaykovsky, M.; Adolph, H. G. *J. Heterocycl. Chem.* **1991**, *28*, 1491.
(15) Eckert, F.; Rauhut, G. *J. Am. Chem. Soc.* **1998**, *120*, 13478.
(16) Eckert, F.; Rauhut, G.; Katritzky, A. R.; Steel, P. J. *J. Am. Chem. Soc.* **1999**, *121*, 6700.
(17) Werner, H.-J.; Knowles, P. J. Contributions from Amos, R. D.; Berning, A.; Cooper, D. L.; Deegan, M. J. O.; Dobbyn, A. J.; Eckert, F.; Hampel, C.; Leininger, T.; Lindh, R.; Lloyd, A. W.; Meyer, W.; Mura, M. E.; Nicklass, A.; Palmieri, P.; Peterson, K.; Pitzer, R.; Pulay, P.; Rauhut, G.; Schütz, M.; Stoll, H.; Stone, A. J.; Thorsteinsson, T. Molpro, Version 98.2 (a package of ab initio programs); University of Birmingham: Birmingham, UK, 1998 (see http://www.tc.bham.ac.uk/molpro/).
(18) Eckert, F.; Pulay, P.; Werner, H. J. *J. Comput. Chem.* **1997**, *18*, 1473.
(19) Eckert, F.; Werner, H. J. *Theor. Chem. Acc.* **1998**, *100*, 21.
(20) Becke, A. D. *J. Chem. Phys.* **1993**, *98*, 5648.
(21) Frisch, M. J.; Trucks, G. W.; Schlegel, H. B.; Gill, P. M. W.; Johnson, B. G.; Robb, M. A.; Cheeseman, J. R.; Keith, T.; Petersson, G. A.; Montgomery, J. A.; Raghavachari, K.; Al-Laham, M. A.; Zakrzewski, V. G.; Ortiz, J. V.; Foresman, J. B.; Cioslowski, J.; Stefanov, B. B.; Nanayakkara, A.; Challacombe, M.; Peng, C. Y.; Ayala, P. Y.; Chen, W.; Wong, M. W.; Andres, J. L.; Replogle, E. S.; Gomperts, R.; Martin, R. L.; Fox, D. J.; Binkley, J. S.; Defrees, D. J.; Baker, J.; Stewart, J. P.; Head-Gordon, M.; Gonzalez, C.; Pople, J. A. Gaussian 94, Revision D.1, Gaussian, Inc.: Pittsburgh, PA, 1995.
(22) Gonzalez, C.; Schlegel, H. B. *J. Chem. Phys.* **1989**, *90*, 2154.
(23) Vosko, S. H.; Wilk, L.; Nusair, M. *Can. J. Phys.* **1980**, *58*, 1200.

(24) Mugnoli, A.; Mariani, C.; Simonetta, M. *Acta Crystallogr*. **1965**, *19*, 367.
(25) Rauhut, G. *J. Comput. Chem.* **1996**, *17*, 1848.
(26) Glukhovtsev, M. N.; Bach, R. D.; Pross, A.; Radom, L. *Chem. Phys. Lett.* **1996**, *260*, 558.
(27) Bell, R. L.; Tavaeras, D. L.; Truong, T. N.; Simons, J. Int. *J. Quantum Chem.* **1997**, *63*, 861.
(28) Kristyan, S.; Pulay, P. *Chem. Phys. Lett.* **1994**, *229*, 175.
(29) Azhary, A. E.; Rauhut, G.; Pulay, P.; Werner, H. *J. Chem. Phys.* **1998**, *108*, 5185.
(30) Schütz, M.; Rauhut, G.; Werner, H. *J. Phys. Chem. A* **1998**, *102*, 5997.
(31) Truhlar, D. G. Direct Dynamics Methods for the Calculation of Reaction Rates. In *The Reaction Path in Chemistry*; Heidrich, D., Ed.; Kluwer: Dordrecht, 1995.
(32) Eckert, F.; Rauhut, G. Unpublished results.
(33) Rauhut, G.; Pulay, P. *J. Phys. Chem.* **1995**, *99*, 3093, 14572(E).
(34) Scott, A. P.; Radom, L. *J. Phys. Chem.* **1996**, *100*, 16502.
(35) El-Azhary, A. A. *J. Phys. Chem.* **1996**, *100*, 15056.
(36) Lee, S. Y.; Boo, B. H. *J. Phys. Chem.* **1996**, *100*, 15073.
(37) Zuilhof, H.; Dinnocenzo, J. P.; Reddy, A. C.; Shaik, S. *J. Phys. Chem.* **1996**, *100*, 15774.
(38) Csonka, G. I.; Nguyen, N. A.; Kolossováry, I. *J. Comput. Chem.* **1997**, *18*, 1534.
(39) Truhlar, D. G.; Garrett, B. C.; Klippenstein, S. J. *J. Phys. Chem.* **1996**, *100*, 12771 and references therein.
(40) Corchado, J. C.; Coitino, E. L.; Chuang, Y.-Y.; Fast, P. L.; Truhlar, D. G. *J. Phys. Chem. A* **1998**, *102*, 2424.
(41) Baboul, A. G.; Schlegel, H. B. *J. Chem. Phys.* **1997**, *107*, 9413.
(42) Pulay, P.; Török, F. *Acta Chim. Acad. Sci. Hung.* **1965**, *47*, 273.
(43) Pulay, P.; Fogarasi, G.; Pongor, G.; Boggs, J.; Vargha, A. *J. Am. Chem. Soc.* **1983**, *105*, 7073.
(44) Rauhut, G.; Jarzecki, A.; Pulay, P. *J. Comput. Chem.* **1997**, *18*, 489.
(45) Gonzales-Lafont, A.; Truong, T. N.; Truhlar, D. G. *J. Chem. Phys.* **1991**, *95*, 8875.